Chemical Engineering Journal 111 (2005) 5–11

Chemical Engineering Journal

www.elsevier.com/locate/cej

Estimation of trickle-to-pulse flow regime transition and pressure drop in high-pressure trickle bed reactors with organic liquids

M.I. Urseanu [a,*], J.G. Boelhouwer [b], H.J.M. Bosman [b], J.C. Schroijen [b], G. Kwant [a]

[a] *DSM Research, P.O. Box 18, 6160 MD Geleen, The Netherlands*
[b] *SABIC EuroPetrochemicals, P.O. Box 319, 6160 AH Geleen, The Netherlands*

Received 16 June 2004; accepted 11 April 2005

Abstract

Flow regime boundaries and pressure drop in trickle bed reactors are crucial for design, scale-up and operation of such reactors. The flow map experiments are performed in a pilot plant reactor of 0.051 m diameter and 1.2 m height, with cumene–hydrogen system. A new technique – the acoustic signal measurement – is used for distinguishing between trickle and pulse flow regimes. The effect of operating pressure was investigated in the pressure range of 0.14–2.0 MPa. For higher operating pressures, the trickle-to-pulse transition boundary moves towards higher flow rates of both liquid and gas phases.

The pressure drop over the reactor bed is increasing with increasing operating pressure and gas/liquid throughputs. The pressure drop results obtained with hydrogen at higher operation pressures match reasonably well the results obtained with air–water at atmospheric pressure. This comparison is made using a new developed pressure drop correlation and illustrates the influence of increased gas density (high operating pressure effect). The Trickle Bed Simulator of University Laval [F. Larachi, B. Grandjean, I. Iliuta, Z. Bensetiti, A. André, G. Wild, M. Chen, Excel Worksheet Simulator for Trickle-Bed Reactors, http://www.gch.ulaval.ca/bgrandjean/pbrsimul/pbrsimul.html, 1999] was found to match reasonably well our pilot plant measured values for low and high operating pressures.

Keywords: Chemical reactors; Multiphase flow; Trickle bed reactor; Hydrodynamics; Flow map; Pressure drop

1. Introduction

Trickle bed reactors are the most widely used type of multiphase reactors. The large applicability and importance of this type of reactors arises from their major use in the petroleum industry for hydroprocessing of medium heavy and heavy oil fractions. Among these applications, trickle bed reactors are also used in biochemical and chemical industries, in wastewater treatment and electrochemical processing. The liquid and gas flow co-currently down through a fixed bed of catalyst particles. The commercial trickle bed reactors operate usually adiabatically, at high temperatures and pressures, and often involve hydrogen and organic liquids. Industrial trickle beds have typically diameters of 2–4 m and heights of 15–25 m. Laboratory and pilot plant experiments used in the development of new processes or optimisation of the existent ones should give accurate results, reliable for design and scale-up. It is an important issue to know what the basic requirements are for using downscaled reactors that lead to meaningful results for integral industrial reactors. This topic is extensively presented in [2].

Knowledge of the flow regime in which the reactor will operate is very important because other hydrodynamic parameters, especially the mass transfer rates, are affected by hydrodynamics differently in each regime. In a trickle bed, various flow regimes are distinguished, depending on gas and liquid properties, throughputs, operating conditions and packing characteristics. The four main flow regimes observed are trickle flow, mist flow, bubble flow and pulsing flow. The flow regime boundaries with respect to gas and liquid flow rates are schematically shown in Fig. 1. Each flow regime corresponds to a specific gas–liquid interaction, thus having a great influence on parameters as liquid hold-up, pressure

* Corresponding author. Tel.: +31 46 4761990; fax: +31 46 4760809.
E-mail address: ioana.urseanu@dsm.com (M.I. Urseanu).

1385-8947/$ – see front matter © 2005 Elsevier B.V. All rights reserved.
doi:10.1016/j.cej.2005.04.015

Nomenclature

d_p	grain equivalent diameter (m)
D_T	column diameter (m)
P	operating pressure (Pa)
$\Delta P/z$	differential pressure drop (Pa/m)
STDEV	standard deviation from pressure drop measurements (–)
T	operating temperature (°C)
U_G	superficial gas velocity (m/s)
U_L	superficial liquid velocity (m/s)

Greek letters

ε_b	bed porosity (–)
η_L	liquid viscosity (Pa s)
ρ_G	gas density (kg/m^3)
σ	surface tension (N/m)

drop and mass and heat transfer rates. The trickle flow regime occurs at relatively low gas and liquid flow rates. The liquid flows as a laminar film and/or in rivulets over the packing particles, while the gas passes through the remaining void space. At high gas and low liquid flow rates, transition to mist flow occurs. The liquid mainly travels down the column as droplets entrained by the continuous gas phase. The bubble flow regime appears at high liquid flow rates and low gas flow rates. In this case, the liquid is the continuous phase and the gas moves in the form of dispersed bubbles. At moderate gas and liquid flow rates, the pulsing flow regime is obtained. This regime is characterized by the successive passage of liquid-rich and gas-rich regions through the bed. While the existence of the various flow regimes in trickle bed reactors is well known and many efforts were done in order to establish a theoretical rule to demarcate the regime boundaries, none

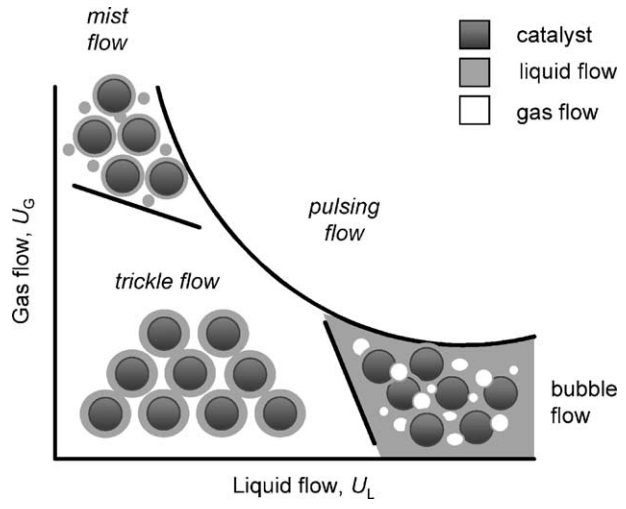

Fig. 1. Schematic illustration of the location of the trickle, mist, bubble and pulsing flow regimes with respect to gas and liquid flow rates.

of them is able at this moment to accomplish such a complex task. Numerous attempts were done to model hydrodynamics of trickle bed reactors. Reviews on published models in this area can be found in [3–5].

As a consequence of gas flow downward through the packed bed, a pressure drop arises over the trickle bed reactor due to friction at the gas–liquid interface. The pressure drop over the column bed is an important design parameter and also essential for sizing the compression equipment. Following the approach used by Lockhart and Martinelli [6] for the pressure drop for two-phase co-current flow in tubes, several relations have been suggested in order to predict the pressure drop for co-current two-phase flow in packed beds. The influence of pressure on the two-phase pressure drop in trickle beds was previously studied by several researchers [3,4,7–13]. In spite of the vast information found in literature on two-phase pressure drop, the vast majority of the correlations are restricted to narrow ranges of operating conditions, properties of the phases and packing characteristics, and their application for large-scale industrial reactors is questionable.

The goals of this study are: (a) to generate the trickle-to-pulse flow regime transition map and (b) to analyse the influence of the operating pressure on the total pressure drop for the cumene–hydrogen system in a pressurised pilot plant reactor.

2. Experimental

2.1. Experimental equipment

Two different set-ups were used for performing the experiments. In Fig. 2(a), the schematic drawing of the pilot plant trickle bed used for the experiments with cumene–hydrogen, at high pressures, is shown. A "Brooks" mass flow controller measured the gas feed rate. The liquid phase is mixed with the gas phase in-line, just before entering the reactor. The trickle bed reactor is made up of CrNi steel and is 0.051 m in diameter and 1.2 m in bed length. The catalyst used is 2 wt.% Pd on extruded carbon from Engelhard, with a nominal particle diameter of 1.5 mm. Properties of the catalyst are given in Table 1. The complete reactor bed used in our experiments contains several layers of inert particles (bed porosity, $\varepsilon_b = 0.4$) besides the catalyst layer ($\varepsilon_b = 0.34$), as shown in

Table 1
Catalyst specifications

Property	Value
Palladium content (wt.%)	2
Bulk density (kg/m^3)	420
Bed porosity (ε_b)	0.34
Particle nominal diameter (m)	1.5×10^{-3}
Surface equivalent grain diameter (d_p) (m)	2.5×10^{-3}
Average extrudate length (m)	3.5×10^{-3}
Particle sphericity factor	0.81
BET (m^2/g)	1100

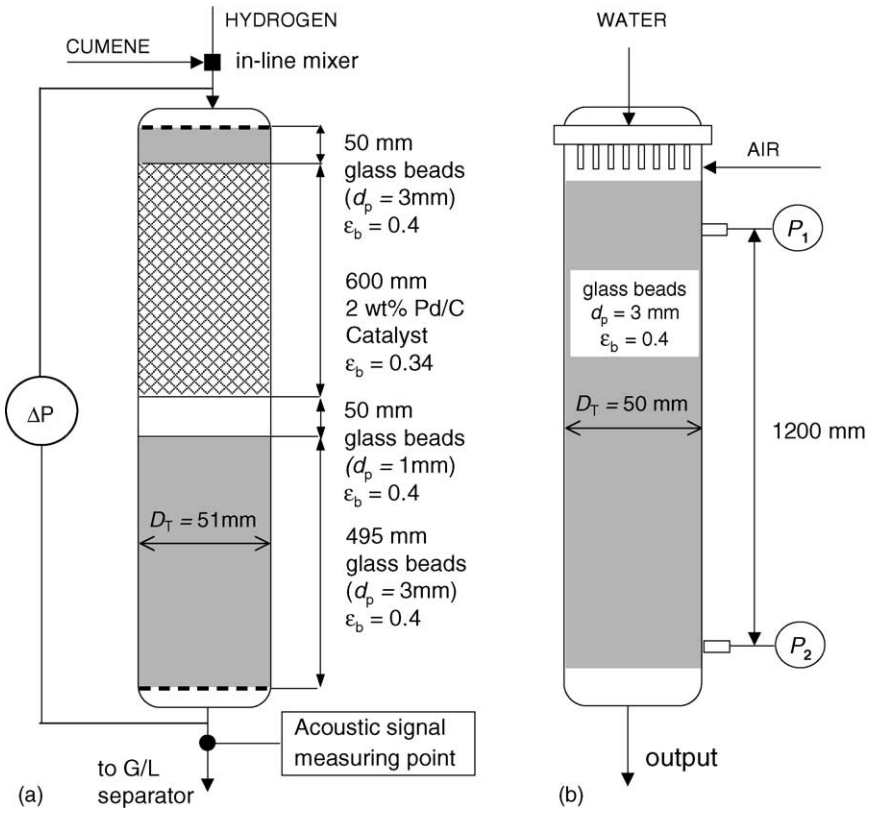

Fig. 2. Schematic view of the experimental equipment: (a) high-pressure experiments with cumene/AMS–hydrogen and (b) air–water experiments.

Fig. 2(a). In the top of the reactor, a first 5 cm layer of 3 mm diameter glass beads is used. This layer ensures a uniform radial distribution of the liquid/gas mixture over the reactor cross-section. The Pd/C catalyst particles bed has a height of 0.6 m. A 5 cm layer of 1 mm diameter glass beads supports the catalyst packing. The last layer contains 3 mm glass beads and has a height of 0.495 m. The entire reactor packing is supported at the bottom of the column by a stainless steel screen. To measure the two-phase pressure drop through the reactor bed, pressure taps were drilled in the reactor head and in the outlet pipe of the reactor and a differential pressure transducer was mounted. For each experiment, the differential pressure drop over the entire reactor bed was measured for 15 min. The output signal of the transducer was fed to an A/D converter and stored in a PC, with a sampling frequency of 0.2 Hz. The experiments were performed at room temperature and the pressure range investigated was 0.14–2.0 MPa. Different superficial gas and liquid velocities were combined, in the range U_G = 0.04–0.2 m/s and U_L = 0.0014–0.016 m/s, respectively. The physical properties of the phases used in the experiments are given in Table 2.

The cold flow experiments were performed in a Plexiglas column of 0.05 m inner diameter (see Fig. 2(b)). As packing material glass beads of 3 mm diameter were used, with a bed porosity ε_b = 0.4 and a specific area of 1200 m^{-1}. The packing was supported at the bottom of the column by a stainless steel screen. Air and water were uniformly distributed at the top of the column. The experiments were conducted at room temperature and atmospheric pressure; see also [14] for more details. Gas and liquid flow rates were measured by calibrated flowmeters. Two pressure taps were installed along the column height and the differential pressure drop, $\Delta P = P_2 - P_1$,

Table 2
Physical properties of the phases

Liquid phase	Temperature, T (°C)	Surface tension, σ (N/m)	Density, ρ_L (kg/m^3)	Viscosity, η_L (mPa s)
Cumene	20	0.0282	863	0.790
Water	20	0.0727	998	1.005

Gas phase	Temperature, T (°C)	Pressure, P (MPa)	Density, ρ_G (kg/m^3)	Viscosity, η_G (mPa s)
Air	20	0.1	1.29	0.017
Hydrogen	20	0.1	0.09	0.008

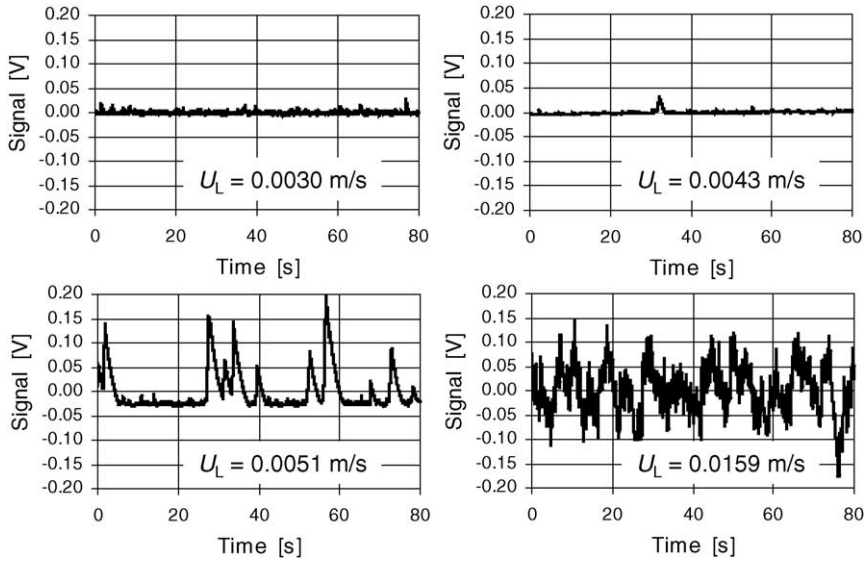

Fig. 3. Recorded acoustic signals at increasing superficial liquid velocity and constant superficial gas velocity, U_G = 0.2 m/s.

was measured for a 1.2 m reactor height. For both set-ups, the standard deviation from the pressure drop signal was used for determination of the trickle-to-pulse transition boundary.

2.2. Acoustic signal measurements

The transition boundary determination for cumene–hydrogen system was also back-upped using a new measurement technique: acoustic signal measurement. Acoustic measurements represent a valuable tool to observe the hydrodynamic behaviour of trickle bed reactors when visual inspection is not possible. Acoustic signals on the output pipe of the reactor were recorded using an "Ultrapobe® 2000", with a frequency of 1000 Hz. The measurements were performed at one pressure, P = 0.2 MPa, room temperature, superficial gas velocities in the range U_G = 0.05–0.2 m/s and liquid flow rate in the range U_L = 0.0014–0.016 m/s.

3. Results and discussion

3.1. Transition from trickle-to-pulse flow

The trickle-to-pulse flow transition determination presented typically in the literature is based on visual determinations for experiments performed in transparent columns. In our case, the pilot plant reactor we used is not transparent; therefore, our method requires a special accuracy check.

The acoustic measurement technique is in fact a measurement of the sound volume due to the flowing liquid. A set of acoustic signals at increasing liquid flow rate and a constant superficial gas velocity of 0.20 m/s is shown in Fig. 3. Pulses are clearly visualised starting with a superficial liquid velocity of 0.0051 m/s, as indicated by the large peaks in the signal. At the highest liquid flow rates, the peaks corresponding to pulses are somewhat chaotic. This may indicate the transition from pulsing flow to bubble flow.

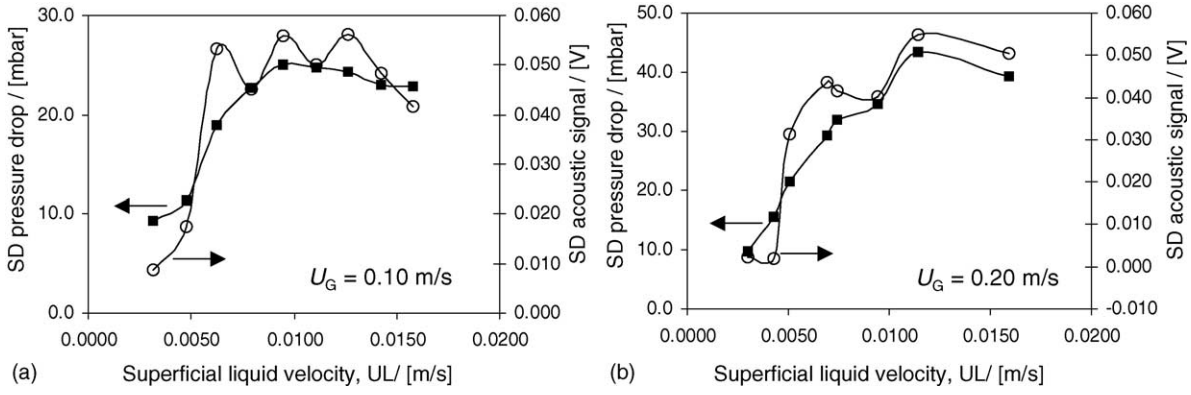

Fig. 4. Comparison between standard deviation from pressure drop and acoustic signals plotted vs. superficial liquid velocities at: (a) U_G = 0.1 m/s and (b) U_G = 0.2 m/s.

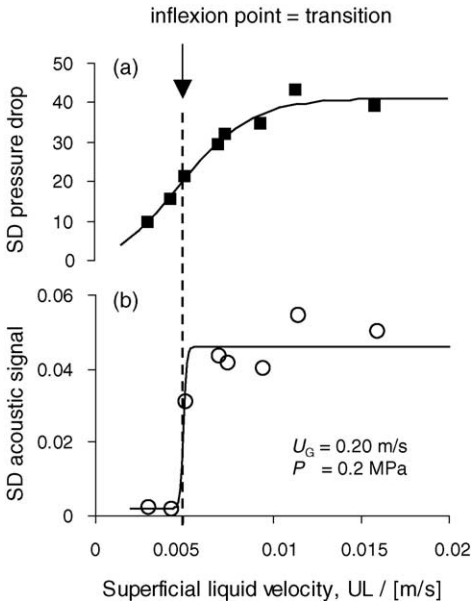

Fig. 5. Transition point determination at $U_G = 0.2$ m/s and $P = 0.2$ MPa using standard deviation from: (a) pressure drop signals and (b) acoustic signals.

In order to establish the transition between trickle to natural pulsing flow, several combinations of gas flow–liquid flow were used. At four different gas flow rates, varying in the range $U_G = 0.05$–0.2 m/s, the liquid flow rate was varied in a broad range. For each experiment, acoustic signals and pressure drop data were recorded for a period of 160 s, respectively, 7 min. From both recorded sets of data, the standard deviation was calculated. Examples of standard deviation values recorded at $U_G = 0.1$ and 0.2 m/s are shown in

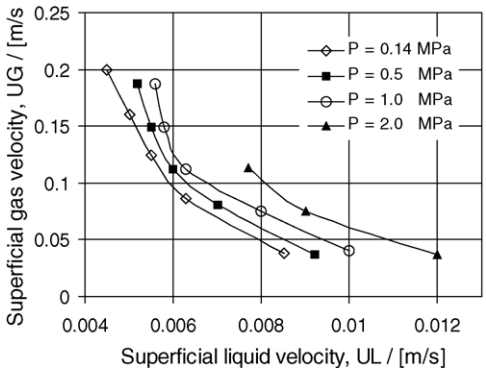

Fig. 6. Trickle-to-pulse flow regime transition for cumene–hydrogen at different operating pressures.

Fig. 4. The standard deviation values plotted versus superficial liquid velocity show for both trends a characteristic "S" shape, increasing with U_L. With changing the flow regime from trickle-to-pulse flow, a sudden transition in the standard deviation value is observed. The regime transition was approximately determined using the inflexion point from each standard deviation curve. Although the two standard deviation curves (obtained from the pressure drop measurements and from the acoustic signals) show some quantitative differences, the inflexion point of both curves is approximately the same. A mathematical function was proposed and fitted to the experimental data for each STDEV curve. The inflexion point was calculated from the analytical solution of the second derivative of the function. The comparison between the values obtained by the two methods is illustrated in Fig. 5. As one can see, the two values are identical.

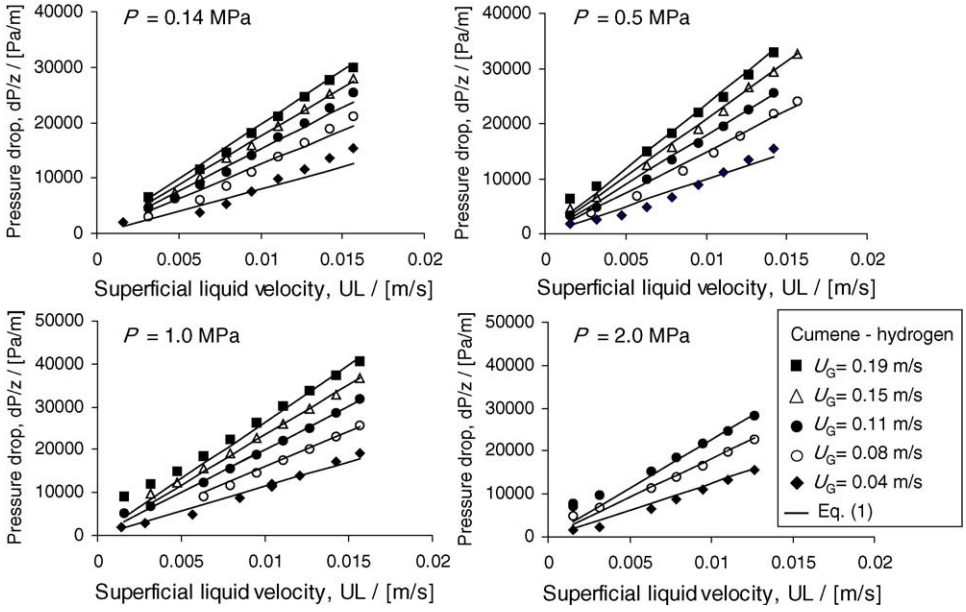

Fig. 7. Pressure drop experimental data for cumene–hydrogen for various flow rates and different operating pressures; comparison with the predictions of Eq. (1).

In order to build up a flow map for cumene–hydrogen at different operation pressures, only pressure drop measurements were performed further, and the method described above to determine the inflexion point was applied. The final results are presented in Fig. 6. The trickle-to-pulse flow regime transition shifts to higher flow rates when higher operating pressures are applied. These results are in agreement with previous findings [9]. Higher density of the gas phase, caused by increasing the reactor pressure, generates higher pressure drop over the packed bed. The pressure drop acts on the liquid flow and dynamic liquid hold-up decreases. As a direct consequence, the liquid film thickness also decreases and therefore, at higher pressures, the liquid film is more difficult to be interrupted, in order to generate pulses.

3.2. Pressure drop

Fig. 7 presents the two-phase pressure drop results obtained with cumene–hydrogen in the pilot plant reactor. The data are presented as a function of the gas and the liquid superficial gas velocities, for different operating pressures. At a given pressure, the pressure drop increases with both flow rates. Increasing the operating pressure, the differential pressure drop also increases, for constant gas–liquid flow conditions. These findings are in accordance to recently published literature [15,16].

For studying the influence of increased gas density (high operating pressure effect), the experimental data obtained with hydrogen as gas phase at high pressures are compared with experiments performed with air–water at atmospheric pressure, in similar reactor conditions. The ranges of pressure drop values are in the same order of magnitude. In order to compare the two sets of data, a simple correlation was developed, which takes into account the operating parameters (superficial gas and liquid velocities, U_G and U_L), the relevant system properties varied in the experiments (liquid viscosity, η_L, and gas density, ρ_G) and the particle (characteristic) diameter, d_p:

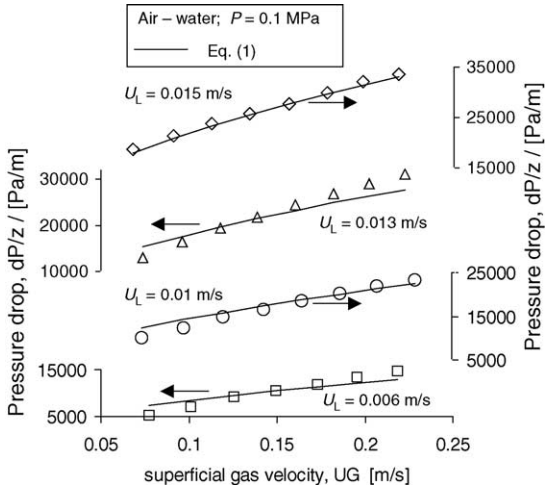

Fig. 8. Air–water pressure drop measured data compared with predictions of Eq. (1).

$$\frac{\Delta P}{z} = 16 U_G^{0.54} U_L \rho_G^{0.17} \eta_L^{0.5} d_p^{-2.76} \quad (1)$$

The pressure drop results obtained with hydrogen at higher operation pressure match reasonably well the results obtained with air at atmospheric pressure (see Figs. 7 and 8), in the range of superficial gas velocities experimented, up to $U_G = 0.2$ m/s. The fact that the use of heavier gases at lower pressures can experimentally simulate hydrodynamics of pressurised systems was also underlined in [5]. The fit parameters in Eq. (1) were determined by multiple regression solver routine of Microsoft Excel 2000 in which the mean-square deviations between experiments and model equations were minimised. Note that Eq. (1) can predict the pressure drop for the specific range of experimental conditions and characteristic geometry mentioned in this work; this model is not advised to be used on general basis (i.e. for other systems and conditions). From the existent literature

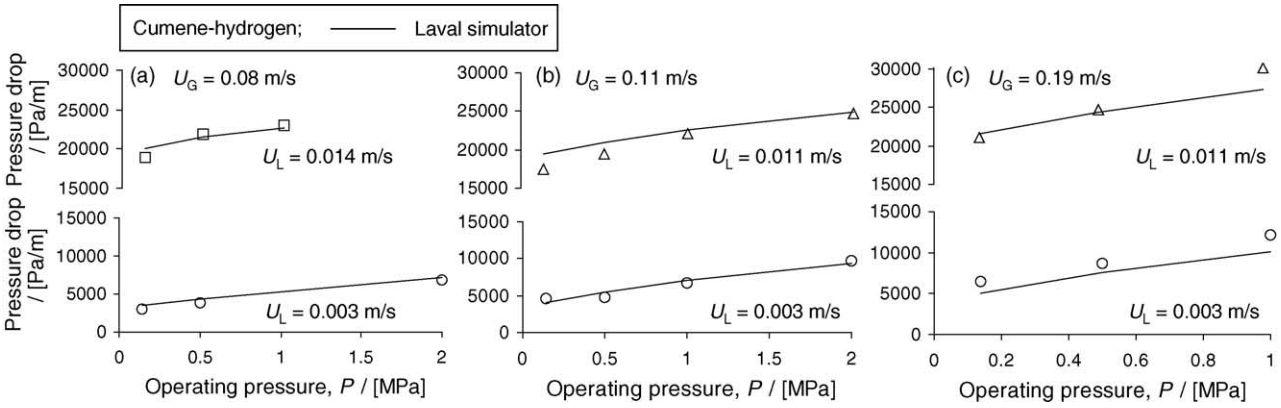

Fig. 9. Influence of operating pressure on total pressure drop for cumene–hydrogen system: (a) $U_G = 0.08$ m/s, (b) $U_G = 0.11$ m/s and (c) $U_G = 0.19$ m/s. Experimental data from this work compared with predictions of Laval simulator (http://www.gch.ulaval.ca/bgrandjean/pbrsimul/pbrsimul.html) [1].

correlations predicting pressure drop in trickle bed reactors, the Trickle bed Simulator of University Laval, http://www.gch.ulaval.ca/bgrandjean/pbrsimul/pbrsimul.html [1], is showing a good match with our measured values for low and high operating pressures (see Fig. 9).

4. Concluding remarks

Trickle-to-pulse flow transition boundaries for hydrogen–cumene system are determined experimentally for different operating pressures in the range of 0.14–2.0 MPa and summarised as a flow map. The transition boundary is obtained using the inflexion point in the standard deviation curve from pressure drop measurements; the technique used was verified by another new technique: the acoustic signal measurements (valuable technique when visualisation is not possible). The boundary between trickle and pulse flow shifts towards higher superficial liquid velocities when the operating pressure increases.

The pressure drop over the reactor bed is increasing with increasing operating pressure and gas/liquid flow rates. The pressure drop results obtained with hydrogen at higher operation pressures match reasonably well the results obtained with air at atmospheric pressure. This comparison illustrates the influence of increased gas density (high operating pressure effect). Compared with existent literature correlations, the Trickle Bed Simulator of University Laval, http://www.gch.ulaval.ca/bgrandjean/pbrsimul/pbrsimul.html [1], is fitting reasonably well our measured values.

Acknowledgement

The authors acknowledge financial support from the European Commission Program “Competitive and Sustainable Growth” under Contract G1RD-CT2000-00225 (European Project “Cyclop”).

References

[1] F. Larachi, B. Grandjean, I. Iliuta, Z. Bensetiti, A. André, G. Wild, M. Chen, Excel Worksheet Simulator for Trickle-Bed Reactors, http://www.gch.ulaval.ca/bgrandjean/pbrsimul/pbrsimul.html, 1999.

[2] S.T. Sie, R. Krishna, Process development and scale up: scale-up and scale-down of trickle bed processes, Rev. Chem. Eng. 14 (1998) 203–252.

[3] M.H. Al-Dahhan, M.P. Dudukovic, Pressure drop and liquid holdup in high pressure trickle-bed reactors, Chem. Eng. Sci. 49 (1994) 5681–5698.

[4] M.H. Al-Dahhan, F. Larachi, M.P. Dudukovic, A. Laurent, High-pressure trickle-bed reactors: a review, Ind. Eng. Chem. Res. 36 (1997) 3292–3314.

[5] M.P. Dudukovic, F. Larachi, P. Mills, Multiphase catalytic reactors: a perspective on current knowledge and future trends, Catal. Rev. 44 (1) (2002) 123–246.

[6] R.W. Lockhart, R.C. Martinelli, Proposed correlation of data for isothermal two-phase, two component flow in pipes, Chem. Eng. Prog. 45 (1949) 39–48.

[7] M.J. Ellman, N. Midoux, A. Laurent, J.C. Charpentier, A new, improved pressure drop correlation for trickle-bed reactors, Chem. Eng. Sci. 43 (1998) 2201–2206.

[8] W.J.A. Wammes, S.J. Mechielsen, K.R. Westerterp, The transition between trickle flow and pulse flow in a cocurrent gas–liquid trickle-bed reactor at elevated pressures, Chem. Eng. Sci. 45 (1990) 3149–3158.

[9] W.J.A. Wammes, K.R. Westerterp, Hydrodynamics in a pressurized co-current gas–liquid trickle bed reactors, Chem. Eng. Technol. 14 (1991) 406–413.

[10] W.J.A. Wammes, J. Middelkamp, W.J. Huisman, C.M. de Baas, K.R. Westerterp, Hydrodynamics in a co-current gas–liquid trickle bed reactor at elevated pressures, AIChE J. 37 (1991) 1849–1862.

[11] F. Larachi, A. Laurent, N. Midoux, G. Wild, Experimental study of a trickle-bed reactor operating at high pressure, Chem. Eng. Sci. 46 (1991) 1233–1246.

[12] G. Wild, F. Larachi, A. Laurent, The hydrodynamic characteristics of co-current downflow and co-current upflow gas–liquid-solid catalytic fixed bed reactors: the effect of pressure, Rev. Inst. Fr. Pt. 46 (1991) 467–490.

[13] R.A. Holub, M.P. Dudukovic, P.A. Ramachandran, A phenomenological model of pressure drop, liquid hold-up and flow regime transition in gas–liquid trickle flow, Chem. Eng. Sci. 47 (1992) 2343–2348.

[14] J. Boelhouwer, Nonsteady operation of trickle-bed reactors, Ph.D. Dissertation in Chemical Engineering, University of Eindhoven, Eindhoven, 2001.

[15] I. Iliuta, B.P.A. Grandjean, F. Larachi, New mechanistic film model for pressure drop and liquid holdup in trickle flow reactors, Chem. Eng. Sci. 57 (2002) 3359–3371.

[16] I. Iliuta, F. Larachi, Magnetohydrodynamics of trickle bed reactors: mechanistic model, experimental validations and simulations, Chem. Eng. Sci. 58 (2003) 297–307.